CHEMISTRY OF MATERIALS

Article

pubs.acs.org/cm

Low-Temperature Atomic Layer Deposition of High Purity, Smooth, Low Resistivity Copper Films by Using Amidinate Precursor and Hydrogen Plasma

Zheng Guo,[†] Hao Li,[‡] Qiang Chen,[†] Lijun Sang,[†] Lizhen Yang,[†] Zhongwei Liu,*[,†] and Xinwei Wang*[,‡]

[†]Laboratory of Plasma Physics and Materials, Beijing Institute of Graphic Communication, Beijing 102600, China

[‡]School of Advanced Materials, Shenzhen Graduate School, Peking University, Shenzhen 518055, China

Supporting Information

ABSTRACT: Agglomeration is a critical issue for depositing copper (Cu) thin films, and therefore, the deposition should be preferably performed below 100 °C. This work explores an atomic layer deposition (ALD) process for copper thin films deposited at temperature as low as 50 °C. The process employs copper(I)-*N*,*N*′-diisopropylacetamidinate precursor and H_2 plasma, which are both highly reactive at low temperature. The deposition process below 100 °C follows an ideal self-limiting ALD fashion with a saturated growth rate of 0.071 nm/cycle. Benefitting from the low process temperature, the agglomeration of Cu thin films is largely suppressed, and the Cu films deposited at 50 °C are pure, continuous, smooth, and highly conformal, with the resistivity comparable to PVD Cu films. In-situ reaction mechanism studies by using quartz crystal microbalance and optical emission spectroscopy are followed, and the results confirm the high reactivity of the Cu amidinate precursor at low temperature. To the best of our knowledge, this is the first successful implementation of metal amidinate precursors for low-temperature (~50 °C) ALD process. The strategy of using metal amidinate precursors in combination with highly reactive H_2 plasma is believed to be extendable for the depositions of other pure metals at low temperature.

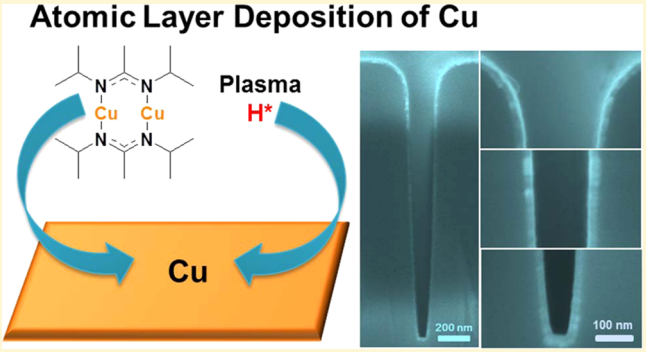

1. INTRODUCTION

Due to the low electrical resistivity and high electromigration resistance, copper (Cu) has been employed as the primary interconnect material in microelectronic devices. As the device size continues to scale down, as well as the quick development of 3D devices, there is an urgent need on fabrication methods to deposit high-quality Cu thin films conformally inside narrow trenches or on sophisticated 3D structures.[1] Atomic layer deposition (ALD) is well known for depositing uniform films conformally on high aspect ratio structures, so it is considered as one of the most important techniques for realizing nanoscale device fabrication.[2−4]

Although many excellent ALD processes have been developed for various materials,[3] the existing ALD processes for Cu metal are not yet completely satisfactory. One critical problem with Cu is its low onset temperature for agglomeration. It has been suggested[5] that the deposition temperature should be lower than 100 °C to avoid the agglomeration, in order to obtain continuous, smooth, thin Cu films. However, as recently surveyed by Barry et al.,[6] most of the reported Cu processes were still performed above 100 °C. Examples with the deposition temperature close to 100 °C include Cu(dmap)$_2$/$ZnEt_2$ (dmap = dimethylamino-2-propoxide) at 100−120 °C,[7] Cu(pyrim)$_2$/$ZnEt_2$ (pyrim = *N*-ethyl-2-pyrrolylaldiminate) at 120−150 °C,[8] Cu(dmamb)$_2$/HCOOH/N_2H_4 (dmamb = dimethylamino-2-methyl-2-butoxide) at 100−170 °C,[5] and Cu(dmap)$_2$/(HCOOH)/BH_3NHMe_2 at 130−160 °C.[9] Besides the deposition temperature issue, these processes also suffered from various other issues, such as Zn impurity incorporation if using $ZnEt_2$,[8] careful handling required for hydrazine, and catalytic Pd substrate is needed if using BH_3NHMe_2.[9] Another combination of Cu(hfac)$_2$/pyridine/H_2 (hfac = 1,1,1,5,5,5-hexafluoroacetylacetonate) was reported to deposit Cu in the temperature range from 100 °C down to room temperature;[10] however, the deposited films tend to contain higher than normal impurities of carbon and oxygen.

In general, the difficulty to achieve low-temperature Cu deposition is mainly due to the lack of suitable precursors that have enough reactivity at low temperature and can proceed the surface reactions in a clean and complete fashion. Notice that the reactivity should be sufficient for both the Cu precursor and the coreactant agent. As for the coreactant agent, an often-used strategy is to use energetic plasma to enhance its reactivity, which is also known as plasma-enhanced ALD (PEALD).

Received: June 6, 2015
Revised: August 13, 2015
Published: August 14, 2015

DOI: 10.1021/acs.chemmater.5b02137
Chem. Mater. 2015, 27, 5988−5996

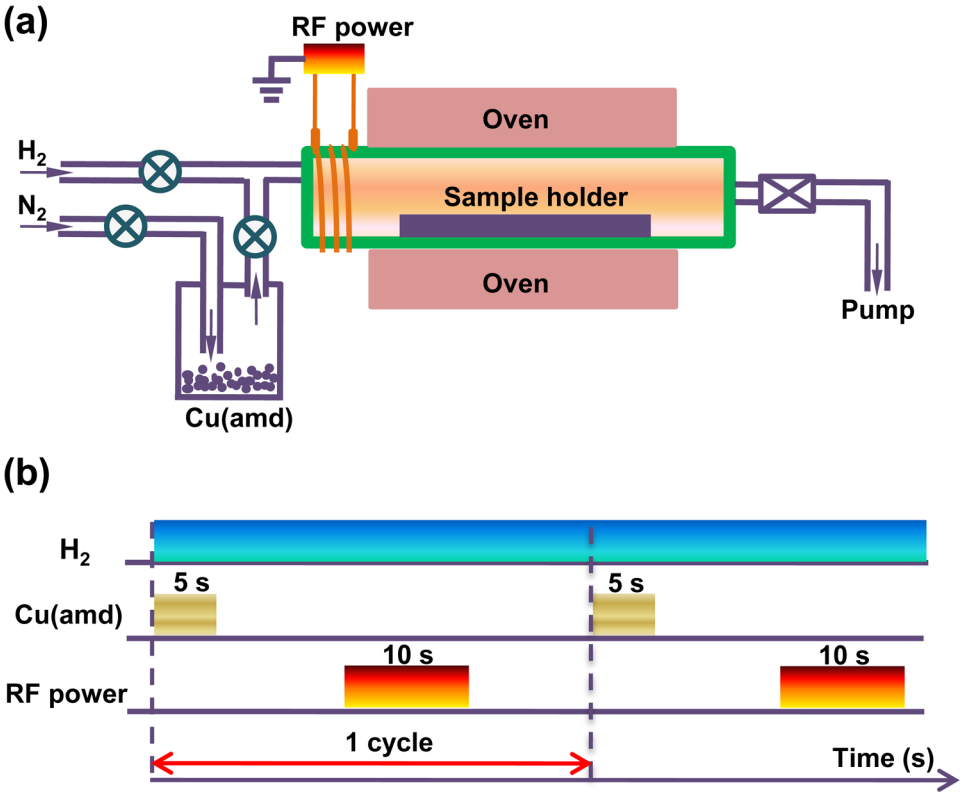

Figure 1. (a) Schematic of the tubular ALD reactor. (b) Schematic layout of the plasma-enhanced ALD cycle for Cu deposition.

Several successful implementations of H_2 plasma for low-temperature ALD processes have been reported with the Cu precursor of $Cu(acac)_2$ (acac = acetylacetonate) at 85−140 °C,[11,12] $Cu(thd)_2$ (thd = 2,2,6,6-tetramethylheptane-3,5-dionate) at 60−180 °C,[13] and $Cu(dmamb)_2$ at 100−180 °C,[14] respectively. H_2 plasma is supposed to generate highly reactive hydrogen atoms that can hydrogenate and eliminate the organic ligands on surface.[15,16] However, not all the hydrogenated products are volatile, so possibly a few percent of carbon and oxygen may still leave in the deposited films as the impurities.[14] On the other hand, the atomic hydrogen does not stick very long on Cu surface;[17] they may quickly recombine into H_2 molecules and leave the Cu surface when the plasma is turned off. So H_2 plasma is unlikely to directly facilitate the following chemisorption step of Cu precursor on freshly formed Cu surface, and as a result, the growth rate may still be low (e.g., only ∼0.02 nm/cycle for $Cu(acac)_2$[11,12] and $Cu(thd)_2$[13]). Therefore, a low-temperature reactive Cu precursor is still largely in need to be used along with the H_2 plasma.

In the process of seeking suitable precursors, metal amidinate compounds have aroused our special attention. Metal amidinates were proposed by Gordon et al.[18] as the ALD precursors to deposit pure metal films by reacting with molecular H_2, and many transition metals (including Cu) have been successfully deposited from the related amidinate precursors. The Cu films deposited from copper(I)-*N*,*N*′-di-*sec*-butylacetamidinate were quite pure,[19] which suggested a favorable clean surface reaction. However, the minimum deposition temperature (>185 °C[18]) was still quite high for Cu, so the resulting Cu films showed considerable agglomeration on SiO_2.[19] Also problematic was its slow saturation behavior,[19] which seemed to indicate some kinetic barriers for this precursor. Therefore, Cu amidinates were not thought to be applicable for <100 °C ALD process before. But recently, some mechanism studies performed by Dai et al.[20] and Ma et al.[21−23] in ultrahigh vacuum (UHV) systems revealed a somewhat different story. Ma et al. found[23] that the copper(I)-*N*,*N*′-di-*sec*-butylacetamidinate molecule was actually quite reactive at low temperature; it could spontaneously dissociate and chemisorb on clean Cu surface at −25 °C, and the actual rate limiting step for the deposition was the dissociation of molecular H_2 into H atoms on Cu surface, as the H atoms were the critical species for hydrogenating the surface organic ligands. This finding is very important and intriguing. It inspires us to think whether the amidinate precursor can be used along with H_2 plasma at low temperature, since the H_2 plasma can provide a rich amount of H atoms so the rate limiting step may be much accelerated.

To implement this idea, we developed a low-temperature Cu ALD process in this work, by employing copper(I)-*N*,*N*′-diisopropylacetamidinate as the Cu source and H_2 plasma as the reducing agent. As speculated, due to the excellent low-temperature reactivity of both species, the deposition process proceeded in an ideal ALD fashion with a reasonably high saturated growth rate (0.071 nm/cycle) even at temperature as low as 50 °C. The films deposited at 50 °C were pure, continuous, and smooth, with the resistivity comparable to PVD Cu films. The Cu films could also be conformally deposited into 10:1 aspect ratio trenches, demonstrating the promising applications of this process for 3D structural microelectronics. In-situ quartz crystal microbalance and optical emission spectroscopy measurements were followed to confirm the high reactivity at low temperature for both reactants. To the best of our knowledge, this is the first report of implementing metal amidinate precursors for low-temperature (∼50 °C)

DOI: 10.1021/acs.chemmater.5b02137
Chem. Mater. 2015, 27, 5988−5996

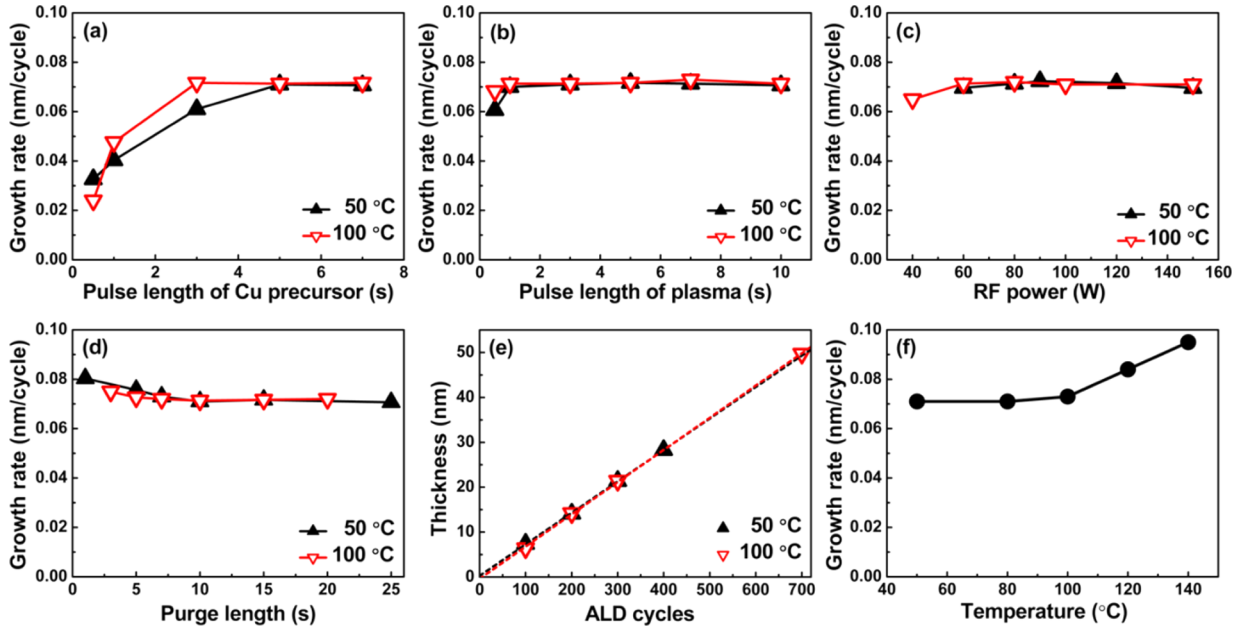

Figure 2. Self-limiting growth behavior is demonstrated at both 50 and 100 °C. (a) and (b) show how the growth rate approach a constant (a) as the pulse length of the Cu precursor increases, and (b) as the pulse length of the plasma increases, respectively. (c) Growth rate as a function of the RF power of the plasma. (d) Growth rate as a function of the purge length after each precursor pulse. (e) Film thickness as a function of the number of ALD cycles; the dashed lines represent the corresponding linear fittings. (f) Growth rate as a function of the deposition temperature. Unless otherwise labeled on the corresponding horizontal axis, the deposition conditions were 5 s, 10 s, 10 s, and 80 W for the Cu(amd) pulse, purge, plasma pulse, and RF power, respectively.

ALD. As metal amidinates generally show clean surface chemistry, we believe that our strategy can be extended to other amidinate based precursors, so that more types of high-quality metals can be deposited at a temperature close to room temperature.

2. EXPERIMENTAL SECTION

ALD Reactor Setup. The deposition was performed in a homemade tubular ALD reactor, which is schematically illustrated in Figure 1a. The deposition chamber was made of a 60 cm long quartz tube, the upstream part of which was wrapped with copper coil. Through this coil, pulsed radiofrequency (RF) power of 13.56 MHz ranging from 40−150 W was supplied to generate plasma inside the upstream zone of the quartz tube. A 40 cm long sample holder was placed in the center zone of the tube, and sample substrates were normally placed near the center of the holder for deposition.

Deposition Details. Copper(I)-*N*,*N*′-diisopropylacetamidinate (Cu(amd)) was used as the Cu precursor. The Cu(amd) was synthesized by a literature method.[24] ^{1}H NMR and thermal gravimetric analysis (Supporting Information Figure S1) were used to confirm the product and its purity. For deposition experiments, the Cu(amd) precursor was kept in a glass container inside an oven at 90 °C, and the precursor vapor was delivered into the deposition chamber with the assist of purified N_2 gas (50 sccm) as the carrier gas. As will be shown in the following, Cu(amd), along with hydrogen plasma, can produce very good Cu films in an ideal self-limiting ALD fashion, but Cu(amd) and H_2 gas do not directly react at our low deposition temperatures (≤100 °C). Thus, in this case, we can safely use pure H_2 gas (50 sccm) as the purging gas for removing excess Cu precursor. Using H_2 gas for purging can also provide particular convenience with our experimental setup, as in the following plasma steps, one only needs to turn on the RF power to generate the hydrogen plasma, but no need to wait for the flow to stabilize as required for switching gas types. A schematic of the ALD cycles is shown in Figure 1b. Lengths of the precursor pulse, purge, and plasma pulse as well as the plasma RF power were varied to determine the saturation growth conditions. We found that (vide infra) a cyclic deposition schedule of 5, 10, 10, and 10 s for the Cu(amd) pulse, purge, plasma pulse, and purge, respectively, with the RF power of 80 W gave out the ideal ALD saturation growth behavior. Thus, unless otherwise specified, we chose to use this set of parameters for the later depositions. Silicon wafers and glass slides were used as the substrates, and no appreciable difference was observed for the films deposited on these two types of substrates. The substrate samples were sequentially cleaned by acetone, methanol, and isopropanol and then pretreated by 3 min of H_2 plasma prior to the Cu deposition. Native oxide on silicon was not intentionally removed.

Film Characterizations. To measure the film thickness, the deposited Cu films were first scratched and then measured the step profiles (Veeco, Dektak 150) across the scratched lines. The obtained thickness values were also verified by X-ray reflectivity (Bruker, D8 Advance) for smooth films and by cross-sectional scanning electron microscopy (SEM) (Hitachi, SU8020) for thick films. The surface morphology of the films was examined by SEM and atomic force microscopy (AFM) (Veeco, diInnova). The film microstructure was examined by transmission electron microscopy (TEM) (JEOL, JEM2100). The composition of the films was analyzed by X-ray photoelectron spectroscopy (XPS) (Thermo Scientific, K-Alpha). The sheet resistance of the films was measured by four-point probes method (RTS-8).

In-Situ Diagnostics. Quartz crystal microbalance (QCM) and optical emission spectrometer (OES) were used to in situ investigate the reaction mechanism. The QCM consisted of a gold-covered AT-cut quartz crystal with an oscillation frequency of ∼6 MHz, and the change of the frequency was monitored by the Inficon SQC-310 controller. The OES spectra were collected by the Acton SepctroPro SP-2500 spectrometer, which had a nominal spectral resolution of 0.05 nm from 200−900 nm. Photomultiplier tube type detector (Hamamatsu) was used for the time-resolved measurements, in which the transient emission signals were acquired by an oscilloscope (Tektronix DP04104) with a temporal resolution of 2 ms.

3. RESULTS

The deposition behavior of using Cu(amd) as the copper source and hydrogen plasma as the reducing agent was carefully

DOI: 10.1021/acs.chemmater.5b02137
Chem. Mater. 2015, 27, 5988−5996

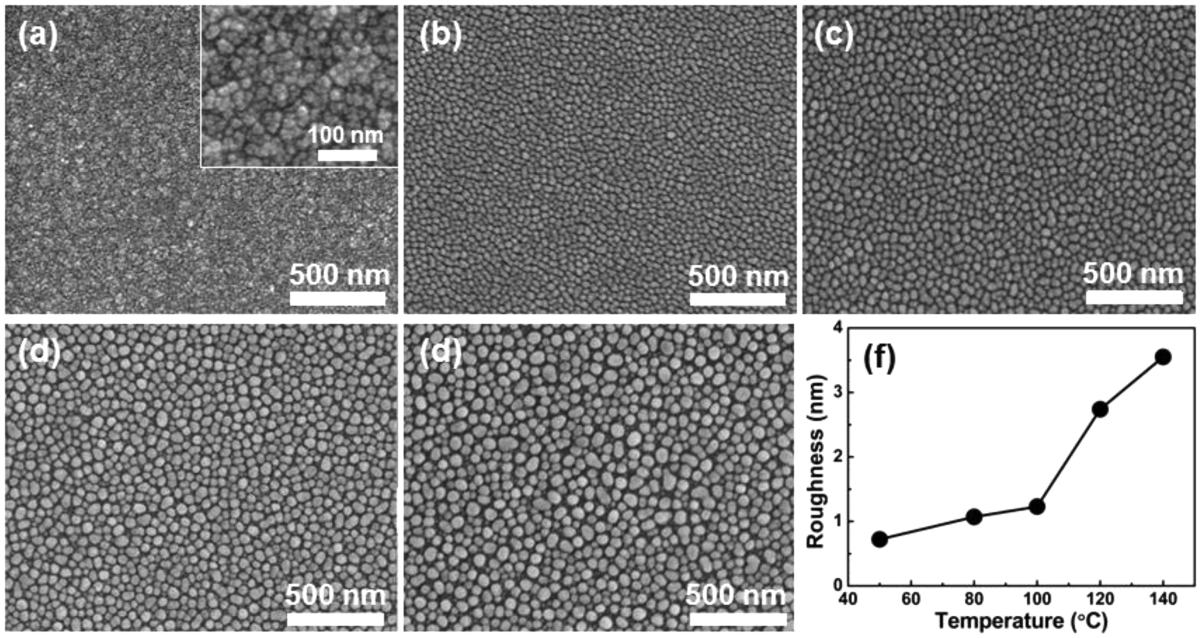

Figure 3. Comparison of the SEM top-view images of the 300-cycle Cu films deposited at (a) 50 °C, (b) 80 °C, (c) 100 °C, (d) 120 °C, and (e) 140 °C, respectively. (f) Plot of the AFM-measured rms roughness values of these films (see Supporting Information Figure S3 for associated AFM images).

studied in the temperature range of 50−140 °C. Excellent ALD-behavior growth was achieved from 50 to 100 °C. Typical ALD-behavior growth curves corresponding to the deposition temperatures of 50 and 100 °C, are shown in Figure 2a−e.

The growth rate versus the pulse length of Cu(amd) typically saturated in several seconds, as shown in Figure 2a. However, this saturation length was, in fact, not well-defined because our Cu precursor remained in solid phase during the deposition so the evaporation rate of the precursor gradually decreased as the small-size precursor crystallites evaporated first and left the large-size crystallites, which could be much slower to evaporate. Consequently, the pulse length required to saturate the growth rate would gradually increase over time. Therefore, the growth rate was always carefully monitored, and excessively long pulses were used to ensure the saturation. On the other hand, the growth rate versus the pulse length of plasma saturated uniformly in about 1 s (Figure 2b), and this value was also consistent with the QCM and OES measurements as will be shown later. The density of the reactive species in the hydrogen plasma was controlled by the supplied RF power. As shown in Figure 2c, as long as enough power was supplied (~60 W), the growth rate did not vary significantly with the RF power. But, if the supplied power was too high, the large amount of highly reactive plasma species could transfer too much energy to the substrate, and therefore raise the substrate temperature, which could considerably accelerate the unwanted agglomeration of the deposited copper thin films (Supporting Information Figure S2). Thus, to keep the agglomeration minimum, we chose to use the RF power of 80 W in the following experiments. The purge length after the Cu precursor pulse was also varied, and the results showed that 10 s of inert gas (H_2) purging was sufficient to remove the excess precursor (Figure 2d). Based on the above results and analysis, we concluded that an excellent ALD saturation growth behavior could be obtained with suitable deposition conditions. A suitable set of the deposition conditions are, for instance, 5 s, 10 s, 10 s, and 80 W for the Cu(amd) pulse, purge, plasma pulse, and RF power, respectively. Unless otherwise specified, we chose to use this set of parameters for the following part of this study.

With the saturation growth conditions, good linear growth behavior was obtained as shown in Figure 2e, and no obvious incubation cycles were observed in the initial growth. The temperature dependence of the growth rate was also investigated. As shown in Figure 2f, the growth rate remained fairly constant at around 0.071 nm/cycle below 100 °C, but increased gradually to 0.095 nm/cycle when the deposition temperature raised to 140 °C. The increase of the growth rate might be due to the partial CVD reaction with H_2 at the elevated temperature.[25] But a more critical issue associated with the elevated temperature is the accelerated agglomeration for the deposited thin copper films. The deposition of thin copper films is known to suffer from easy agglomeration,[19] as the copper metal has rather poor adhesion to most oxide substrates and the surface copper atoms are quite mobile at an elevated temperature.[26,27] This temperature effect was also observed in our experiments. As shown in Figure 3, where the surface morphology and roughness of the 300-cycle copper films deposited at various temperatures were compared, continuous films were only obtained for the depositions performed at 50 °C; at 80 °C, the films were barely continuous, and ≥100 °C clearly discontinuous island-like films were formed. Also, the grain size (or island size) increased along with the deposition temperature, which again suggested that the deposition temperature was the critical factor for agglomeration. Notice that the obtained upper limit of the deposition temperature to form continuous films in this study was appreciably lower than the upper limit suggested previously[5] (more than 20 °C lower). This is probably because we used the energetic plasma which could locally heat up the substrate and enhance the mobility of surface copper atoms during the deposition. In fact, we found that increasing the RF power could also result in larger grain size (Supporting Information Figure S2). Nevertheless, the films deposited at 50 °C looked quite good; the films were continuous and fairly smooth with an rms roughness of only

DOI: 10.1021/acs.chemmater.5b02137
Chem. Mater. 2015, 27, 5988−5996

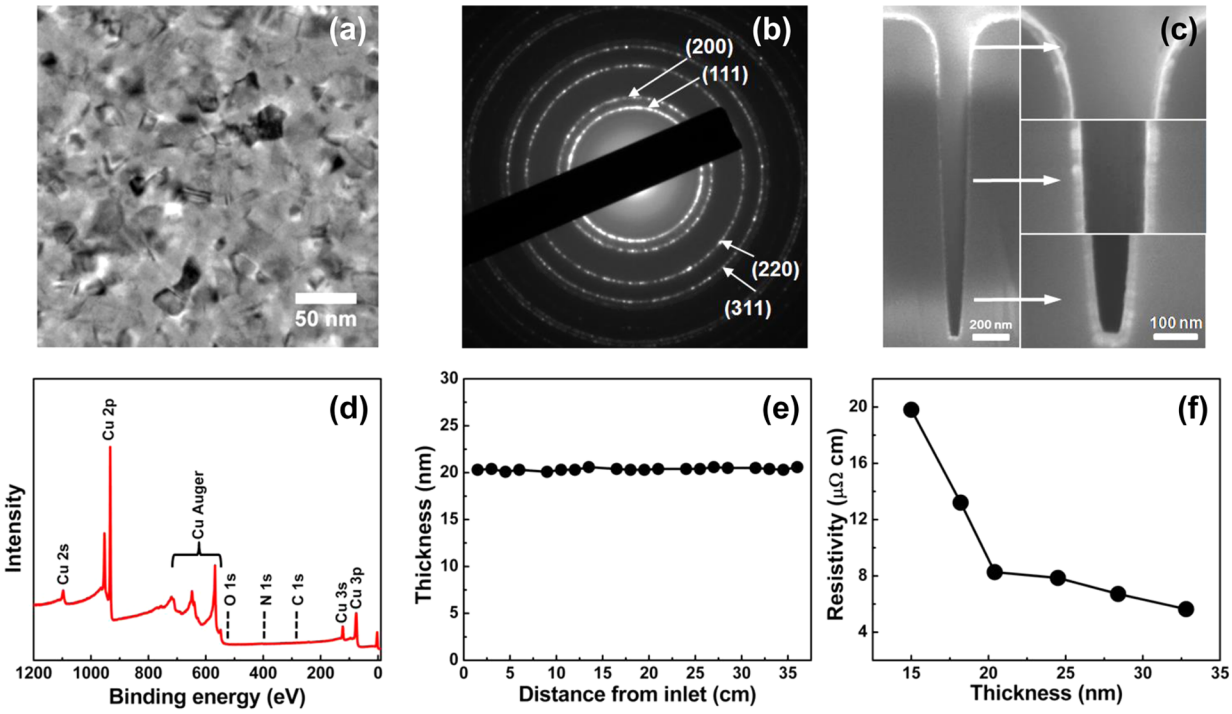

Figure 4. Characterizations of the ~20 nm Cu films deposited at 50 °C, including (a) TEM image and (b) electron diffraction pattern showing the film microstructure; (c) cross-sectional SEM image showing the conformality of the deposition inside a 10:1 trench; (d) XPS spectrum showing the film purity; (e) distribution of the film thickness along the reactor tube; and (f) film resistivity as a function of the film thickness.

0.72 nm as shown in Figure 3f. Therefore, we focused on the films deposited at this temperature for the following characterizations.

The quality of the Cu films deposited at 50 °C was carefully evaluated (Figure 4). The microstructures of the deposited films were examined by TEM. As the TEM image and the associated electron diffraction pattern shown in Figure 4a–b, the deposited Cu films were continuous and polycrystalline with the grain size around 20 nm. The film purity was examined by XPS. After 30 s of Ar^+ sputtering for removing the surface adventitious carbon, no oxygen, nitrogen, or carbon peaks were observed in the XPS spectrum (Figure 4d), indicating the high purity of the deposited Cu films. The film step coverage was evaluated by depositing the Cu film on a trench-structured sample with the aspect ratio of 10:1 for the trenches. As the cross-sectional SEM shown in Figure 4c shows, the Cu film deposited inside the trench was highly conformal, and uniform film thickness was achieved along the entire trench, which demonstrated an excellent step coverage of this ALD process. Large-scale deposition uniformity was evaluated by examining the thickness of films deposited at various places along the reactor tube. As shown in Figure 4e, the film thickness was quite uniform along over 30 cm of the deposition zone, demonstrating a fairly good large-scale deposition uniformity. The resistivity was also measured for the films with various thicknesses. As shown in Figure 4f, the resistivities were all below 20 $\mu\Omega$ cm for the Cu films thicker than 15 nm (compared to the bulk Cu resistivity of 1.7 $\mu\Omega$ cm). Particularly, for the ~33 nm film, the resistivity was only ~5.6 $\mu\Omega$ cm, which was similar to that for a sputtered Cu film with the same thickness (5–6 $\mu\Omega$ cm[28]), indicating that our deposited Cu films had a high purity and low surface roughness, because otherwise the film resistivity would be considerably higher. In addition, the deposited Cu films also passed the Scotch tape test, demonstrating very good adhesion.

From all the aspects of properties we evaluated, the Cu films prepared by our ALD process at 50 °C exhibited very high quality, demonstrating the high promise of this process. On the other hand, this process has an intriguingly uncommon feature that the deposition temperature was appreciably lower than the precursor temperature (50 °C vs 90 °C). Normally, this would result in the precursor condensation effect, where a large amount of precursor could condense on the substrate at lower temperature and become difficult to remove during the purging. To further investigate this regard, as well as to understand the mechanism of the surface reactions involved in this ALD process, we performed the in situ measurements of QCM and OES as the following.

QCM has been frequently used to monitor the growth process of ALD because the oscillation frequency of the quartz crystal is highly sensitive to the mass change. However, the oscillation frequency also depends on temperature, and thus, sometimes, spike-like artifacts due to the sudden temperature changes during pulsing could occur.[29] The situation becomes even more pronounced and complicated when plasma is used, because the charged energetic plasma could not only transfer heat but also interfere with the oscillation circuits.[30] Therefore, special cares were taken for the QCM measurements as well as for the data interpretation. Though our goal was to investigate the ALD process with the cyclic deposition schedule of 5, 10, 10, and 10 s for the Cu(amd) pulse, purge, plasma pulse, and purge, respectively, we first started with the dummy cycles (i.e., without dosing Cu(amd)) until the acquired QCM data reached stable (no baseline drifting), and then followed by the normal deposition cycles. This arrangement allowed the QCM to stabilize at a new temperature due to the heating effect

DOI: 10.1021/acs.chemmater.5b02137
Chem. Mater. 2015, 27, 5988–5996

from the intermittent plasma. A representative set of the acquired QCM data are plotted in Figure 5a, where the last five

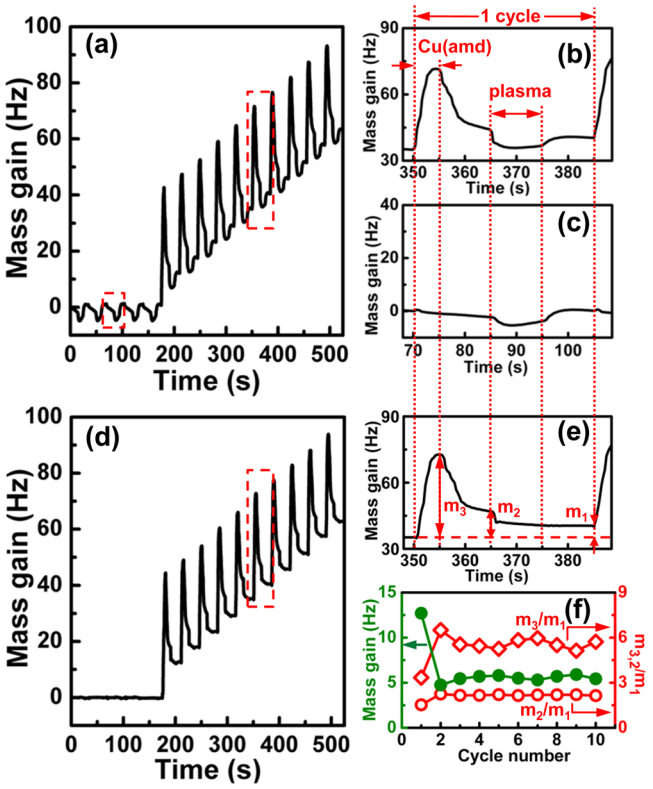

Figure 5. QCM measurements during ALD of Cu at 50 °C. (a) Curve of the acquired mass gain versus the deposition time for five dummy cycles followed by 10 normal ALD cycles. Enlarged curves of two boxed regions in (a) for a normal cycle and a dummy cycle are plotted in (b) and (c), respectively. By removing the plasma effect, the mass gain curves shown in (a) and (b) are updated as (d) and (e), respectively. (f) Plot of the cyclic mass gain of m_1 (green full circles) and the ratios of m_2/m_1 (red open circles) and m_3/m_1 (red open diamonds), where the definitions of m_1, m_2, and m_3 are illustrated in (e).

dummy cycles prior to the deposition were also included for comparison. The mass gain at the end of each ALD cycle showed a clear linear increase with the cycle number. However, the shape of the curve during each ALD cycle was rather convoluted by the plasma effect. For a better comparison, enlarged curves of a typical deposition cycle and a typical dummy cycle are plotted in Figure 5b and c, respectively. The concurrences of the dip shape during the plasma-on stage and the bump shape after the plasma-on stage in both plots indicated that these shapes were the results of the plasma effect. Therefore, to remove the plasma effect, we took the curve shape from the dummy cycles as the background, and subtracted it from the original QCM data. The processed QCM curve is shown in Figure 5d, with a typical deposition cycle enlarged in Figure 5e. As one can see, the artifacts induced by the plasma was successfully eliminated.

The curve shown in Figure 5e exhibits many intriguing features. During the first 5 s when the Cu precursor was supplied, the mass gain of QCM continued increasing to m_3, suggesting that the chemisorption and possibly physisorption of the Cu(amd) precursor occurred on the surface. Then, the mass gain dropped gradually to m_2 during the following 10 s of purging, suggesting that the some adsorbed species could be purged away. The purgeable species were likely those weakly physisorbed precursor dimer molecules and also possibly from the recombination of the chemisorbed precursor monomers. Next, when the plasma was turned on, a steep drop of the mass gain was observed in the initial ~1 s, and then the mass gain remained almost constant until the end of the ALD cycle (m_1). The drop of the mass gain was probably due to the hydrogenation reaction that removed the organic ligands on surface and left only Cu atoms, which had a smaller mass. This reaction probably completed in about 1 s, as the steep drop in mass gain lasted only for that period of time. To facilitate the later discussion on the reaction mechanism, we extracted the m_1, m_2, and m_3 for each ALD cycle, and plotted the m_1 and the ratios of m_2/m_1 and m_3/m_1 as shown in Figure 5f. Except for the first cycle which was strongly affected by the substrate surface, for the following cycles, the ratios of m_2/m_1 and m_3/m_1 remained fairly constant at 2.2 and 5.7, respectively. Noticing that the molecular weight ratio of Cu(amd) and Cu is 3.22, the ratio of m_2/m_1, which fell between 1 and 3.22, indicated that some dissociative chemisorption must occur along with the production of some volatile species. In fact, the detailed mechanism involved in the surface reaction is quite complex, and indeed it is not possible to accurately obtain the whole picture solely by the QCM measurements, but, thanks to Ma et al.[22,23] who have carefully studied a similar compound (copper(I)-*N*,*N*′-di-*sec*-butylacetamidinate) on Cu surface, we can comparatively analyze our results with their results and draw insightful conclusions (see Discussion). In addition, we may assume that $(m_3 - m_2)/m_1$ (i.e., 3.5 in this case) is correlated with the layers of the physisorbed Cu(amd) molecules (possibly sit in the dimeric form outside the chemisorbed layer) on each deposited Cu atom, and according to our data, only about one such layer was expected, indicating the absence of severe precursor condensation with our experimental conditions.

OES is another useful tool to study a plasma system, as many excited gas species in plasma have their own characteristic emission wavelengths. However, the emission spectrum collected during our deposition (Supporting Information Figure S4) was overwhelmed by the strong emissions from atomic H* (e.g., H_α at 656.3 nm) and molecular H_2* (e.g., Fulcher-α $d^3\Pi_u \rightarrow a^3\Sigma_g^+$ bands at 590−640 nm,[31] $G^1\Sigma_g^+ \rightarrow B^1\Sigma_u^+$ bands at 453−464 nm,[32] etc.). The emissions from the expected hydrocarbon/hydroaminocarbon byproducts were probably too weak to be observed, so the time-resolved OES spectra were only taken for the hydrogen species, that is, H* and H_2*. The OES results (Supporting Information Figures S4 and S5) suggested that an appreciable amount of atomic hydrogen was consumed during the first ~1 s when the plasma was on and the consumption of atomic hydrogen depended on the precursor pulse length and saturated at 5 s, which manifested again the self-limiting growth behavior as indicated by Figure 2a.

4. DISCUSSION

Achieving low-temperature Cu ALD generally requires two conditions: (1) the Cu precursor needs to be reactive enough at low temperature to be chemisorbed on the substrate surface, so that an ALD cycle can be initiated; (2) in the second half of an ALD cycle, the organic component of the chemisorbed species needs to be removed by a clean and efficient way, so that the next ALD cycle can proceed. In this work, we employed highly

DOI: 10.1021/acs.chemmater.5b02137
Chem. Mater. 2015, 27, 5988−5996

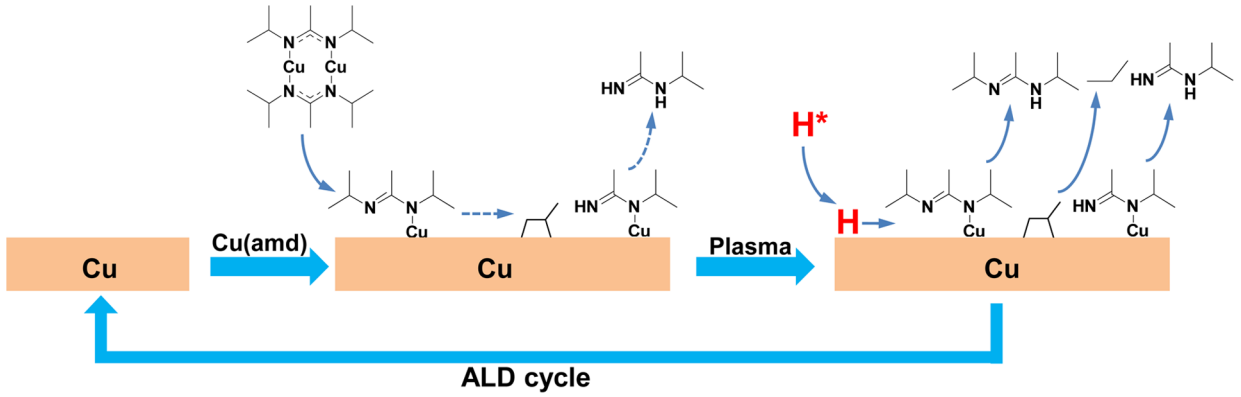

Figure 6. Schematic depiction of the proposed ALD reaction mechanism, where the dash arrows are used to denote partial conversions.

reactive Cu(amd) precursor along with H_2 plasma to fulfill both the requirements. As the results shown previously, benefited from the low process temperature of 50 °C that minimized the agglomeration, very high quality Cu films were obtained. In particular, the deposited films were fairly smooth, continuous, low resistive, and highly conformal, demonstrating the high promise of this process for conformal Cu thin film deposition on 3D structures. On the other hand, the surface chemistry involved in the deposition process must be favorable for obtaining the high quality films. Therefore, we discuss on this regard in the following.

In general, metal amidinates are an interesting class of ALD precursors, as they have quite a few unique features that are considered preferable for depositing pure metals. For instance, the amidinate ligands contain only the elements of C, N, and H, so there is no need for concern about the oxygen incorporation. This is particularly important for a low-temperature plasma-assisted process, because oxygen-containing moieties are likely to be hydrogenated by the plasma to form alcohols and water, which are less volatile than alkanes/amines/ammonia and therefore difficult to be completely purged away at low temperature. On the other hand, the bidentate amidinate ligands also provide enough stability to the coordinated compound, so the Cu(amd) molecule is thermally quite stable below 100 °C. This is also very important because it guarantees that, during the deposition at 50 °C, the physisorbed Cu(amd) molecules do not self-decompose and therefore can be removed as a whole during the following purging steps.

As for the dissociative chemisorption process, Ma et al.[22,23] have carefully studied a similar Cu amidinate compound (i.e., copper(I)-*N*,*N*′-di-*sec*-butylacetamidinate, denoted as Cu(Buamd) in the following) by combined the experiments of temperature-programmed desorption and X-ray photoelectron spectroscopy in an UHV system, and revealed that the Cu(Buamd) can be dissociatively chemisorbed on fresh Cu surface and partially decompose to form *sec*-butyl and *N*-*sec*-butylacetamidinate moieties, with a portion of the latter desorbed from the surface at room temperature. We expect that the surface chemistry involved for our Cu(amd) precursor (i.e., copper(I)-*N*,*N*′-diisopropylacetamidinate) should be similar. During the deposition processed at 50 °C, the chemisorbed Cu(amd) molecules are expected to partially decompose to form isopropyl and *N*-isopropylacetamidinate moieties on Cu surface. If we further assume that some surface *N*-isopropylacetamidinate moieties can desorb from the surface as well, then the desorbed portion can be estimated from the m_2/m_1 ratio from the QCM results. Based on our data, the desorbed portion of the *N*-isopropylacetamidinate moieties was estimated to be 65% (counted based on the total amount of the original *N*,*N*′-diisopropylacetamidinate moieties). This value was fairly high, and it indicated a favorable surface chemistry, because, otherwise, too many bulky amidinate moieties on surface would block the surface reaction sites and result in low deposition rate. In fact, the saturated ALD growth rate in our case was ∼0.071 nm/cycle, which corresponded to about 6 Cu atoms deposited per 1 nm^2 surface area for each ALD cycle. Considering the fact that the surface *N*,*N*′-diisopropylacetamidinate and *N*-isopropylacetamidinate moieties occupy the surface area of roughly 1.0 nm × 0.4 nm and 0.6 nm × 0.4 nm, respectively, it would be impossible to accommodate six amidinate surface moieties within 1 nm^2 area. Therefore, it is fairly reasonable to expect a large portion of the decomposed *N*-isopropylacetamidinate moieties to release from the surface in the chemisorption step. On the other hand, the unreleased *N*-isopropylacetamidinate moieties were unlikely to further decompose at our low process temperature of 50 °C.

After the above complex decomposition and desorption process, a compact chemisorption layer consisting of the undecomposed *N*,*N*′-diisopropylacetamidinate, isopropyl, and unreleased *N*-isopropylacetamidinate surface moieties was likely formed. This layer was compact enough to prevent additional Cu(amd) molecules from approaching the Cu surface, and therefore, further surface chemistry reaction was stopped. Although additional Cu(amd) molecules might still continue to pile up (probably in the dimeric form) on top of the chemisorption layer and form a physisorption layer, as manifested as the difference of $m_3 - m_2$ from the QCM results, this physisorbed layer could be easily removed in the following purging step, so the self-limiting behavior was still perfectly preserved.

As shown in previous XPS results (Figure 2d), the deposited Cu films contained very low impurity level, which suggested that all the surface moieties in the chemisorption layer could be completely hydrogenated in the second half of an ALD cycle, provided that rich amount of atomic hydrogen was supplied from the H_2 plasma. The hydrogenated products were probably propane, *N*-isopropylacetamidine, and *N*,*N*′-diisopropylacetamidine, which were all fairly volatile and could be completely removed by sufficient purging.

As a summary, the proposed ALD reaction mechanism is schematically depicted in Figure 6. The involved surface reactions are regarded as clean reactions, as they allow the entire process to proceed in an ideal ALD fashion and produce high-quality thin films.

DOI: 10.1021/acs.chemmater.5b02137
Chem. Mater. 2015, 27, 5988−5996

5. CONCLUSIONS

In this work, we developed a low-temperature Cu ALD process by employing the highly reactive copper(I)-*N*,*N*′-diisopropylacetamidinate precursor along with the H_2 plasma. The deposition process proceeded in an ideal self-limiting ALD fashion with a reasonably high saturated growth rate of 0.071 nm/cycle below 100 °C. The process temperature could even be as low as 50 °C, so the critical agglomeration issue associated with the Cu thin films was largely suppressed. The Cu films deposited at 50 °C were pure, continuous, smooth, and highly conformal, with the resistivity comparable to PVD Cu films, demonstrating the high promise of this process for microelectronic applications. In-situ QCM and OES measurements were followed to understand the reaction mechanism, and the results confirmed the high reactivity at low temperature for both reactants. To the best of our knowledge, this is the first report of implementing metal amidinate precursors for low-temperature (~50 °C) ALD. As metal amidinates generally show clean surface chemistry, we believe that the strategy of using them in combination with H_2 plasma can be largely generalized and extended to other metal amidinate precursors for depositing various high-quality metal thin films at low temperature.

■ ASSOCIATED CONTENT

Supporting Information

The Supporting Information is available free of charge on the ACS Publications website at DOI: 10.1021/acs.chemmater.5b02137.

Thermal gravimetric analysis of the synthesized Cu(amd) precursor, SEM images of the films deposited with different RF power, AFM images of the films deposited at various temperatures, and time-resolved OES results. (PDF)

■ AUTHOR INFORMATION

Corresponding Authors

*E-mail: liuzhongwei@bigc.edu.cn.
*E-mail: wangxw@pkusz.edu.cn.

Author Contributions

Z. G. and H. L. contributed equally to this work.

Notes

The authors declare no competing financial interest.

■ ACKNOWLEDGMENTS

This work was financially supported by NSFC (Grant Nos. 51302007, 11175024, and 11375031), Shenzhen Science and Technology Innovation Committee (Grant Nos. JCYJ20130329181509637 and JCYJ20140417144423201), and the Importation and Development of High-Caliber Talents Project of Beijing Municipal Institutions (Grant Nos. CIT&TCD201404130 and KM201510015002). X.W. would like to thank Professor Roy G. Gordon at Harvard University for valuable discussion and support.

■ REFERENCES

(1) International Technology Roadmap for Semiconductors. http://www.itrs.net/ (accessed July 2015).
(2) George, S. M. Atomic Layer Deposition: An Overview. *Chem. Rev.* **2010**, *110*, 111−131.
(3) Miikkulainen, V.; Leskela, M.; Ritala, M.; Puurunen, R. L. Crystallinity of Inorganic Films Grown by Atomic Layer Deposition: Overview and General Trends. *J. Appl. Phys.* **2013**, *113*, 021301.
(4) Johnson, R. W.; Hultqvist, A.; Bent, S. F. A Brief Review of Atomic Layer Deposition: From Fundamentals to Applications. *Mater. Today* **2014**, *17*, 236−246.
(5) Knisley, T. J.; Ariyasena, T. C.; Sajavaara, T.; Saly, M. J.; Winter, C. H. Low Temperature Growth of High Purity, Low Resistivity Copper Films by Atomic Layer Deposition. *Chem. Mater.* **2011**, *23*, 4417−4419.
(6) Gordon, P. G.; Kurek, A.; Barry, S. T. Trends in Copper Precursor Development for CVD and ALD Applications. *ECS J. Solid State Sci. Technol.* **2015**, *4*, N3188−N3197.
(7) Lee, B. H.; Hwang, J. K.; Nam, J. W.; Lee, S. U.; Kim, J. T.; Koo, S.-M.; Baunemann, A.; Fischer, R. A.; Sung, M. M. Low-Temperature Atomic Layer Deposition of Copper Metal Thin Films: Self-Limiting Surface Reaction of Copper Dimethylamino-2-propoxide with Diethylzinc. *Angew. Chem., Int. Ed.* **2009**, *48*, 4536−4539.
(8) Vidjayacoumar, B.; Emslie, D. J. H.; Clendenning, S. B.; Blackwell, J. M.; Britten, J. F.; Rheingold, A. Investigation of $AlMe_3$, BEt_3, and $ZnEt_2$ as Co-reagents for Low-Temperature Copper Metal ALD/Pulsed-CVD. *Chem. Mater.* **2010**, *22*, 4844−4853.
(9) Kalutarage, L. C.; Clendenning, S. B.; Winter, C. H. Low-Temperature Atomic Layer Deposition of Copper Films Using Borane Dimethylamine as the Reducing Co-reagent. *Chem. Mater.* **2014**, *26*, 3731−3738.
(10) Kang, S.-W.; Yun, J.-Y.; Chang, Y. H. Growth of Cu Metal Films at Room Temperature Using Catalyzed Reactions. *Chem. Mater.* **2010**, *22*, 1607−1609.
(11) Wu, L.; Eisenbraun, E. Hydrogen Plasma-Enhanced Atomic Layer Deposition of Copper Thin Films. *J. .Vac. Sci. Technol., B* **2007**, *25*, 2581−2585.
(12) Niskanen, A.; Rahtu, A.; Sajavaara, T.; Arstila, K.; Ritala, M.; Leskelä, M. Radical-Enhanced Atomic Layer Deposition of Metallic Copper Thin Films. *J. Electrochem. Soc.* **2005**, *152*, G25−G28.
(13) Jezewski, C.; Lanford, W. A.; Wiegand, C. J.; Singh, J. P.; Wang, P.-I.; Senkevich, J. J.; Lu, T.-M. Inductively Coupled Hydrogen Plasma-Assisted Cu ALD on Metallic and Dielectric Surfaces. *J. Electrochem. Soc.* **2005**, *152*, C60−C64.
(14) Moon, D.-Y.; Han, D.-S.; Shin, S.-Y.; Park, J.-W.; Kim, B. M.; Kim, J. H. Effects of the Substrate Temperature on the Cu Seed Layer Formed Using Atomic Layer Deposition. *Thin Solid Films* **2011**, *519*, 3636−3640.
(15) Profijt, H. B.; Potts, S. E.; van de Sanden, M. C. M.; Kessels, W. M. M. Plasma-Assisted Atomic Layer Deposition: Basics, Opportunities, and Challenges. *J. Vac. Sci. Technol., A* **2011**, *29*, 050801.
(16) Ten Eyck, G. A.; Senkevich, J. J.; Tang, F.; Liu, D.; Pimanpang, S.; Karaback, T.; Wang, G. C.; Lu, T. M.; Jezewski, C.; Lanford, W. A. Plasma-Assisted Atomic Layer Deposition of Palladium. *Chem. Vap. Deposition* **2005**, *11*, 60−66.
(17) Johansson, M.; Lytken, O.; Chorkendorff, I. The Sticking Probability for H_2 on Some Transition Metals at a Hydrogen Pressure of 1 bar. *J. Chem. Phys.* **2008**, *128*, 034706.
(18) Lim, B. S.; Rahtu, A.; Gordon, R. G. Atomic Layer Deposition of Transition Metals. *Nat. Mater.* **2003**, *2*, 749−754.
(19) Li, Z.; Rahtu, A.; Gordon, R. G. Atomic Layer Deposition of Ultrathin Copper Metal Films from a Liquid Copper(I) Amidinate Precursor. *J. Electrochem. Soc.* **2006**, *153*, C787−C794.
(20) Dai, M.; Kwon, J.; Halls, M. D.; Gordon, R. G.; Chabal, Y. J. Surface and Interface Processes During Atomic Layer Deposition of Copper on Silicon Oxide. *Langmuir* **2010**, *26*, 3911−3917.
(21) Ma, Q.; Guo, H.; Gordon, R. G.; Zaera, F. Uptake of Copper Acetamidinate ALD Precursors on Nickel Surfaces. *Chem. Mater.* **2010**, *22*, 352−359.
(22) Ma, Q.; Guo, H.; Gordon, R. G.; Zaera, F. Surface Chemistry of Copper(I) Acetamidinates in Connection with Atomic Layer Deposition (ALD) Processes. *Chem. Mater.* **2011**, *23*, 3325−3334.

DOI: 10.1021/acs.chemmater.5b02137
Chem. Mater. 2015, 27, 5988−5996

(23) Ma, Q.; Zaera, F.; Gordon, R. G. Thermal Chemistry of Copper(I)-N,N′ -di-sec-butylacetamidinate on Cu(110) Single-Crystal Surfaces. *J. Vac. Sci. Technol., A* **2012**, *30*, 01A114.
(24) Li, Z.; Barry, S. T.; Gordon, R. G. Synthesis and Characterization of Copper(I) Amidinates as Precursors for Atomic Layer Deposition (ALD) of Copper Metal. *Inorg. Chem.* **2005**, *44*, 1728−1735.
(25) Krisyuk, V.; Aloui, L.; Prud'homme, N.; Sarapata, B.; Senocq, F.; Samelor, D.; Vahlas, C. CVD of Pure Copper Films from a Novel Amidinate Precursor. *ECS Trans.* **2009**, *25*, 581−586.
(26) Russell, S. W.; Rafalski, S. A.; Spreitzer, R. L.; Li, J.; Moinpour, M.; Moghadam, F.; Alford, T. L. Enhanced Adhesion of Copper to Dielectrics via Titanium and Chromium Additions and Sacrificial Reactions. *Thin Solid Films* **1995**, *262*, 154−167.
(27) Yang, C.-Y.; Chen, J. S. Investigation of Copper Agglomeration at Elevated Temperatures. *J. Electrochem. Soc.* **2003**, *150*, G826−G830.
(28) Barnat, E. V.; Nagakura, D.; Wang, P.-I.; Lu, T.-M. Real Time Resistivity Measurements During Sputter Deposition of Ultrathin Copper Films. *J. Appl. Phys.* **2002**, *91*, 1667−1672.
(29) Rocklein, M. N.; George, S. M. Temperature-Induced Apparent Mass Changes Observed During Quartz Crystal Microbalance Measurements of Atomic Layer Deposition. *Anal. Chem.* **2003**, *75*, 4975−4982.
(30) Heil, S. B. S.; van Hemmen, J. L.; van de Sanden, M. C. M.; Kessels, W. M. M. Reaction Mechanisms During Plasma-Assisted Atomic Layer Deposition of Metal Oxides: A Case Study for Al_2O_3. *J. Appl. Phys.* **2008**, *103*, 103302.
(31) Fantz, U.; Heger, B. Spectroscopic Diagnostics of the Vibrational Population in the Ground State of H_2 and D_2 Molecules. *Plasma Phys. Controlled Fusion* **1998**, *40*, 2023−2032.
(32) Goyette, A. N.; Jameson, W. B.; Anderson, L. W.; Lawler, J. E. An Experimental Comparison of Rotational Temperature and Gas Kinetic Temperature in a H_2 Discharge. *J. Phys. D: Appl. Phys.* **1996**, *29*, 1197−1201.

DOI: 10.1021/acs.chemmater.5b02137
Chem. Mater. 2015, 27, 5988−5996